Proceeding of the 2004 American Control Conference
Boston, Massachusetts June 30 - July 2, 2004

A Practical Solution to the String Stability Problem in Autonomous Vehicle Following

Guang Lu and Masayoshi Tomizuka
Department of Mechanical Engineering,
University of California at Berkeley, Berkeley, CA 94720-1740
glu@me.berkeley.edu tomizuka@me.berkeley.edu

Abstract

This paper describes an improved autonomous vehicle following control scheme based on inter-vehicle communication. A previously developed autonomous following algorithm uses an on-board laser scanning radar sensor (LIDAR) to measure the ego-vehicle's relative position with respect to its preceding vehicle, and the steering command is calculated for the ego-vehicle to follow the preceding vehicle. In this control scheme, the performance of the following vehicle largely depends on the behavior of the preceding vehicle. String stability becomes a serious issue when this control algorithm is applied to a platoon of vehicles. The deterioration of road tracking performance is another concern. The road tracking error of one vehicle is passed on to following vehicles, and the errors may accumulate as they propagate in the upstream direction. It is shown in the paper that inter-vehicle communication is a practical solution to this problem. Experimental and simulation results are presented.

1 Introduction

Intelligent vehicle control has been an active research area in recent years. An important topic in this research field is steering control. The goal of vehicle steering control is to keep the vehicle in its lane by controlling the vehicle's steering angle at the tires. This control objective can be realized by commanding the vehicle either to follow the lane centerline directly or to follow a preceding vehicle. In either way, steering control requires regulation of the vehicle's lateral deviation.

Road-following algorithms rely on certain on-board sensors, such as vision sensors and magnetometers, to detect the vehicle's lateral deviation from the road centerline. Clearly, these control schemes have to rely on certain road infrastructure, e.g. lane markers and magnetic markers. The main benefit of the autonomous vehicle following approach is that it does not require road infrastructure. In autonomous following control, the lateral controller sets the steering command according to the vehicle's relative position with respect to the preceding vehicle. Previous research on autonomous following control can be found in [2][3][5]. It should be noted that the performance of the following vehicle in autonomous following scheme largely depends on the behavior of the preceding vehicle, if no other information on vehicle's lateral deviation from the road is available to the ego-vehicle. This aspect of the autonomous following may constitute a severe string stability problem if the algorithm is applied to a platoon of many vehicles, since the tracking errors of the following vehicles are generally larger than the preceding vehicles, and the errors may accumulate in the upstream direction in the platoon. It also places significant limitations on the performance of autonomous following control even for small groups of vehicles. This problem for autonomous following has not been analyzed in the previous research.

The paper first introduces the autonomous vehicle following problem by describing the vehicle dynamics. Next it shows that a platoon of several vehicles under autonomous following control can be considered as an interconnected system. The string stability of the system can be analyzed using existing definition and theorems about interconnected systems. Then, it is shown that using inter-vehicle communication can change the system into a weakly coupled system, and hence inter-vehicle communication is a practical solution to the string stability problem. The paper also explains the controller design techniques and uses experimental and simulation results to illustrate the effectiveness of the new control scheme.

2 Autonomous Vehicle Following Problem

This paper considers only front-wheel-steered vehicles. The bicycle model is used for analysis and design

0-7803-8335-4/04/$17.00 ©2004 AACC

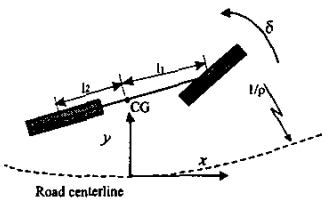

Figure 1: Bycicle model

of control laws. The model is depicted in Fig.1. It retains only the lateral and yaw motions, and neglects motions in other directions [4]. The model may be represented by the following state equation:

$$\dot{x} = Ax + B\delta + W\rho \tag{1}$$

$$x = \begin{pmatrix} y_{CG} & \dot{y_{CG}} & \epsilon_r & \dot{\epsilon_r} \end{pmatrix}^T \tag{2}$$

where x is the state variable, δ is the front wheel steering angle, and ρ is the road curvature (disturbance). y_{CG} is the lateral deviation at the vehicle CG(Center of Gravity), and ϵ_r is the relative yaw of the vehicle sprung mass relative to the road reference frame, respectively. The system matrices are

$$A = \begin{pmatrix} 0 & 1 & 0 & 0 \\ 0 & -\frac{a_{11}}{\dot{x}} & a_{11} & \frac{a_{12}}{\dot{x}} \\ 0 & 0 & 0 & 1 \\ 0 & -\frac{a_{41}}{\dot{x}} & a_{41} & \frac{a_{42}}{\dot{x}} \end{pmatrix} \tag{3}$$

$$B = \begin{pmatrix} 0 \\ b_{21} \\ 0 \\ b_{41} \end{pmatrix} \tag{4}$$

$$W = \begin{pmatrix} 0 \\ w_{21} \\ 0 \\ w_{41} \end{pmatrix} \tag{5}$$

$$a_{11} = (\phi_1 + \phi_2), a_{12} = \phi_1(d_s - l_1) + \phi_2(d_s + l_2) \tag{6}$$

$$a_{41} = \frac{l_1 C_{\alpha_f} - l_2 C_{\alpha_r}}{I_z} \tag{7}$$

$$a_{42} = \frac{l_1 C_{\alpha_f}(d_s - l_1) + l_2 C_{\alpha_r}(d_s + l_2)}{I_z} \tag{8}$$

$$b_{21} = \phi_1, b_{41} = \frac{l_1 C\alpha_f}{I_z} \tag{9}$$

$$w_{21} = -\frac{{l_1}^2 C_{\alpha_f} + {l_2}^2 C_{\alpha_r}}{I_z} \tag{10}$$

$$w_{41} = \phi_2 l_2 - \phi_1 l_1 - \dot{x}^2 \tag{11}$$

The physical meaning and values of the symbols used in the paper are listed in Table 1.

Table 1: Vehicle Parameters

Symbols	Physical Meaning	Value
m	mass	$1485kg$
L	relative longitudinal distance between vehicles	$5m$
d	distance of rear bumper to CG	$2.1m$
I_z	yaw moment of inertia	2872 kg/m^2
C_f	front wheel cornering stiffness	42000 N/rad
C_r	rear wheel cornering stiffness	42000 N/rad
l_1	distance between front wheel and the CG	$1.1m$
l_2	distance between rear wheel and the CG	$1.58m$

The controlled vehicle is equipped with a laser scanning radar sensor (LIDAR). The LIDAR sensor emits laser beams, and detects the returned laser beams after they hit a reflective object. The distance to an object is measured by the Time-of-Flight (TOF) principle, which says:

$$distance = flight\ time \times speed\ of\ the\ light \tag{12}$$

where the speed of the light is 2.976×10^8 m/s. Since the laser beams scan the horizontal plane with constant steps, the orientation of the object can also be measured. In autonomous vehicle following, a reflective target surface is fixed on the rear bumper of each preceding vehicle; therefore the relative distance between every two adjacent vehicles can be measured by LIDAR. A data processing algorithm as described in [5] is used to process the measurements from the LIDAR sensor, and the process also transforms measurements from polar coordinates into Cartesian coordinates. The lateral measurement from LIDAR of the ith vehicle can be represented as

$$y_{Li} = C_2 x_i - C_1 x_{i-1} \tag{13}$$

where x_i denotes the state variable of the ith vehicle, and

$$C_2 = \begin{pmatrix} 1 & 0 & L & 0 \end{pmatrix} \tag{14}$$

$$C_1 = \begin{pmatrix} 1 & 0 & -d & 0 \end{pmatrix} \tag{15}$$

It is clear from the above equations that the platoon that consists of the lead and the following vehicles becomes an interconnected system. For this interconnected system, stability of each system component cannot guarantee the stability of the entire system because the system components are not independent. Instead, string stability needs to be considered.

3 String Stability in Autonomous Following

The following definitions and theorems are borrowed from Swaroop and Hedrick [6]. Consider the following interconnected system:

$$\dot{x}_i = f(x_i, x_{i-1}, \cdots, x_{i-r+1}) \tag{16}$$

where $i \in N$, $x_{i-j} \equiv 0$, $\forall i \leq j$, $x \in R^n$,

$$f: \underbrace{R^n \times \cdots \times R^n}_{r \text{ times}} \rightarrow R^n \quad \text{and } f(0, \cdots, 0) = 0.$$

Definition 1: The origin $x_i = 0$, $i \in N$ of (16) is string stable, if given any $\epsilon > 0$, there exists a $\delta > 0$ such that $||x_i(0)||_\infty < \delta \Rightarrow sup_i ||x_i(\cdot)||_\infty < \epsilon$.

Definition 2: The origin $x_i = 0$, $i \in N$ of (16) is asymptotically (exponentially) string stable if it is string stable and $x_i(t) \rightarrow 0$ asymptotically (exponentially) for all $i \in N$.

Theorem (Weak Coupling Theorem for String Stability): If the following conditions are satisfied:

- f is globally Lipschitz in its arguments, i.e.,

$$\begin{aligned} &|f(y_1, \cdots, y_r) - f(z_1, \cdots, z_r)| \\ \leq &l_1|y_1 - z_1| + \cdots + l_r|y_r - z_r|. \end{aligned} \tag{17}$$

- The origin of $\dot{x} = f(x, 0, \cdots, 0)$ is globally exponentially stable.

Then for sufficiently small l_i, $i = 2, \cdots, r$, the interconnected system is globally exponentially string stable.

The above theorem provides a sufficient condition for string stability of an interconnected system, and it shows that string stability can be achieved if the coupling between the system components is sufficiently weak.

For the steering control of the ith vehicle in autonomous vehicle following, the feedback signal is the vehicle's lateral distance from the preceding vehicle. Hence, by neglecting the road curvature,

$$\dot{x}_i = Ax_i + B\delta_i \tag{18}$$

$$\delta_i = -Ky_{Li} \tag{19}$$

where K is the steering controller. According to Eqn.(13),

$$\delta_i = -K(C_2 x_i - C_1 x_{i-1}) \tag{20}$$

Then,

$$\begin{aligned} \dot{x}_i &= Ax_i + B(-K(C_2 x_i - C_1 x_{i-1})) \\ &= (A - BKC_2)x_i + BKC_1 x_{i-1} \\ &= g(x_i, x_{i-1}) \end{aligned} \tag{21}$$

It is clear from the above equations that the feedback control system of the ith vehicle is coupled with that of the $(i-1)$th vehicle, and hence the vehicle platoon forms an interconnected system. It can be shown that

$$\begin{aligned} &|g(y_1, y_2) - g(z_1, z_2)| \\ \leq &|A - BKC_2| \cdot |y_1 - z_1| + |BKC_1| \cdot |y_2 - z_2| \end{aligned} \tag{22}$$

The above expression shows that to make the coupling weak, the magnitude of the controller K has to be sufficiently small. Clearly, this is not a practical solution.

According to Eqn.(13), if the absolute position of the rear end of the $(i-1)$th vehicle $C_1 x_{i-1}$ is known, the coupling between the ith and the $(i-1)$th vehicle vanishes. Measurements of $C_1 x_{i-1}$ may become available to the $(i-1)$th vehicle, if the vehicle is equipped with appropriate sensors such as GPS, vision camera, or magnetometers. Then through inter-vehicle communication, measurements of a leading vehicle, e.g.the $(i-1)$th vehicle, are shared by all the following vehicles. Define a new system output for the ith vehicle as

$$y_i = y_{Li} + C_1 x_{i-1} = C_2 x_i \tag{23}$$

Note that y_i is the lateral deviation, at a point with distance L ahead of vehicle CG, relative to the road centerline, and it does not depend on the preceding vehicle. Now the following vehicle may use y_i as the feedback signal to the control algorithm, and thus the tracking performance of the vehicle should not depend on that of the preceding vehicle.

4 Controller Design

The control algorithm is required to calculate the correct steering angle at the tires in order to keep the vehicle close to the road centerline according to this new feedback input, regardless of the unknown road curvature and sensor noise. The steering input should be kept small considering the saturation problems and passenger discomfort. Thus, the controller design procedure is based on H_∞ synthesis techniques. As shown in Fig.2, G is used to represent the vehicle lateral dynamics described in Section 2, the road curvature is treated as a unknown disturbance d, n denotes the sensor noise, and the weighting functions W_p, W_n, W_u, and W_d are used to place suitable weights in various frequency ranges. e_p and e_u are the weighted

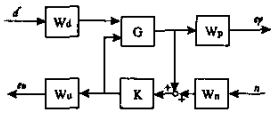

Figure 2: Controller synthesis structure

vehicle lateral deviation and steering input, respectively. The goal of this design is to minimize the effects of the external disturbances d and n on the weighted system outputs in terms of the H_∞ norm.

The weighting functions are chosen according to standard considerations. Penalty on the lateral error should be high at low frequencies for good tracking performance, and low at high frequencies for robustness. Penalty on the steering input should be set low at low frequencies and set high at high frequencies. W_n and W_d are set constant to avoid producing a high-order controller, and they are chosen according to the system performance requirements. The weighting functions chosen for this design are as follows.

$$W_d = \frac{7}{200} \tag{24}$$

$$W_n = \frac{1}{50} \tag{25}$$

$$W_p = 0.1\frac{s+1}{s+0.003} \tag{26}$$

$$W_u = 2000\frac{s+10}{s+120} \tag{27}$$

5 Experimental Setup

A platoon of two Buick vehicles are used in the experimental testing on a test track at the Richmond Field Station, University of California at Berkeley. The maximum allowable speed on the test track is 25MPH. The track consists of many curves, but no preview of the road curvature was used in the testing. The unique feature of this track is that there are equally-spaced magnetic markers buried under the road centerline. Both test vehicles are equipped with two sets of magnetometers, one under the front bumper and the other under the rear bumper. The magnetometers can detect the magnetic field generated by the magnetic markers, and hence they can measure the vehicles' lateral deviation relative to the road centerline. Both vehicles were manually driven in the longitudinal direction, and the space between the two vehicles was controlled manually by the driver who operated the following vehicle. Measurements from the magnetometers on the following vehicle were never used to set the steering control input, but they were collected to evaluate the tracking performance. Inter-vehicle communication between the vehicles was achieved through Utilicom radios. At constant time steps (every $20msec$), the lead vehicle sent its measurements of the rear magnetometers (under rear bumper) to the following vehicle. The lead vehicle was under automatic steering control with the magnetometer measurements as control feedback, but the following vehicle used only LIDAR measurements and communicated information from the lead vehicle.

6 Experimental Results

Figures 3 and 4 show the experimental results of the autonomous vehicle following control without using any inter-vehicle communication. The measurements from each vehicle's front and rear magnetometers are used to show their deviation from the road centerline. Both vehicles traveled up to 20MPH during the testing. The maximum tracking error of the lead vehicle was about $10cm$ from the road centerline, and the maximum tracking error of the following vehicle was about $25cm$ from the road centerline. It can be seen from the results that the lateral error of the following vehicle was positive most of the time, but it can also be seen that the lateral distance measured by LIDAR was negative during the same time (the two signals have opposite sign definitions in experiments). This suggests that this might not be all due to the bias in LIDAR calibration (mainly for LIDAR orientation). It is computed that the average of the lateral deviation of the lead vehicle was about $5cm$, and this could be a reason for the positive bias in the tracking error of the following vehicle. It is clear that without information of the vehicle's position relative to the road centerline, autonomous following algorithm can not adjust the bias in real time.

The experimental results of the autonomous vehicle following control with inter-vehicle communication are shown in Fig. 5 and Fig. 6. The results show that with inter-communication not only the lateral deviation of the following vehicle was significantly reduced, but also the bias disappeared. Note that the speed of the test vehicles was up to 25MPH, a little higher than that in the previous tests. These results show that inter-vehicle communication effectively provides information of the vehicle's position with respect to the road centerline, and the communicated information is useful in reducing the vehicle's lateral deviation and eliminating any real-time bias.

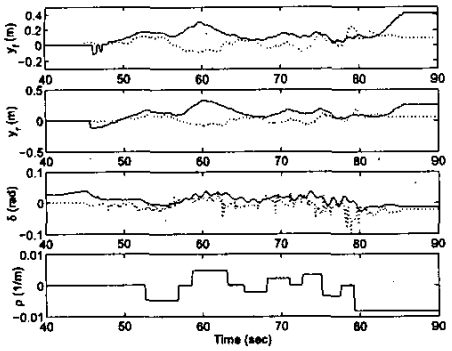

Figure 3: Experimental results for autonomous vehicle following without inter-vehicle communication: front, rear magnetometer outputs, steering angle, and road curvature. (solid: following vehicle; dashed: lead vehicle)

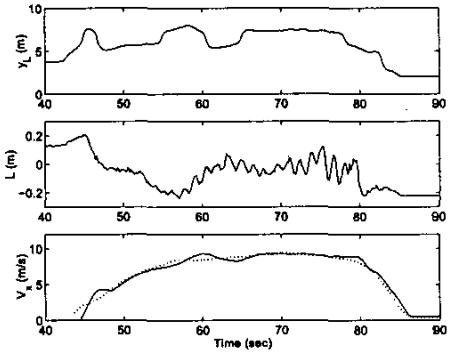

Figure 4: Experimental results for autonomous vehicle following without inter-vehicle communication: lateral, longitudinal distance between the two test vehicles measured by LIDAR, and vehicle speed (solid: following vehicle; dashed: lead vehicle)

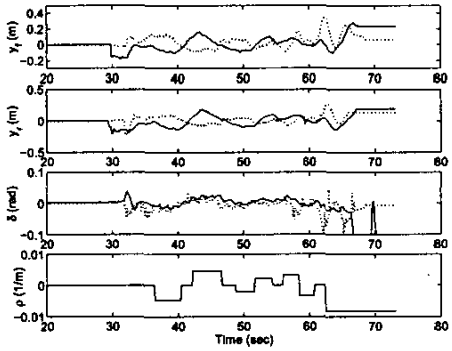

Figure 5: Experimental results for autonomous vehicle following with inter-vehicle communication: front, rear magnetometer outputs, steering angle, and road curvature. (solid: following vehicle; dashed: lead vehicle)

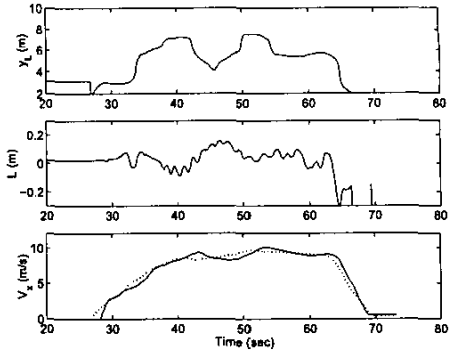

Figure 6: Experimental results for autonomous vehicle following with inter-vehicle communication: lateral, longitudinal distance between the two test vehicles measured by LIDAR, and vehicle speed (solid: following vehicle; dashed: lead vehicle)

7 Simulation for a Vehicle Platoon

Simulations have been conducted to study the effects of inter-vehicle communication on vehicle performance and string stability issues for a larger vehicle platoon. Assuming the 1st vehicle measures its absolute deviation y_{R1} and communicates it to the 2nd vehicle, the 2nd vehicle calculates C_2x_2 by combining the communicated information with LIDAR measurements. A Kalman estimator is developed to estimate y_{R2} from C_2x_2. Then, the estimated $\hat{y_{R2}}$ can be communicated to the 3rd vehicle, and the 3rd vehicle calculates C_3x_3 by combining $\hat{y_{R2}}$ with LIDAR measurements y_{L3}. Similar algorithms can be applied to all the other following vehicles.

The simulation used a platoon of four vehicles, and the simulated road consists of two curves with curvature $\pm\frac{1}{800m}$ respectively. All vehicles were running at same speed in the simulation. The simulation results with and without communication are shown in Fig.7 and Fig.8 respectively. The results show that with inter-vehicle communication, the lateral errors of the all the following three vehicles are almost the same, and they no longer accumulate in the upstream direction of the platoon.

8 Conclusions

This paper has presented a new scheme for the steering control of a passenger vehicle from an autonomous vehicle following approach. Autonomous vehicle following allows a vehicle to automatically follow the trajectory of its preceding vehicle, based on real-time

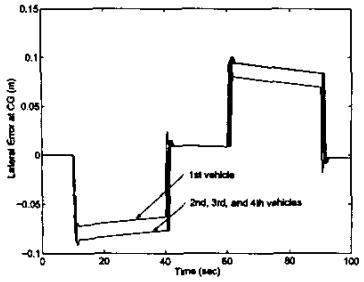

Figure 7: Simulation results for a platoon of four vehicles with perfect estimation

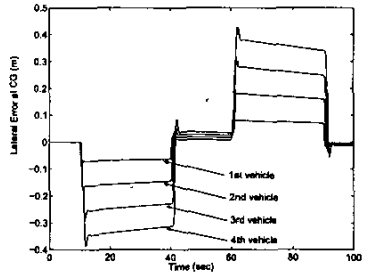

Figure 8: Simulation results for autonomous vehicle following control without inter-vehicle communication (for a platoon of four vehicles)

information of the relative distance between the two vehicles. This paper has analyzed the string stability issues for the autonomous following approach, and suggested using inter-vehicle communication to solve the problem. The controller used measurements from an on-board laser scanning radar sensor (LIDAR) and communicated lateral deviation of the lead vehicle. Experimental and simulation results have been presented and they show that inter-vehicle communication has effectively reduced the vehicle tracking errors in autonomous following.

Acknowledgement

This work was supported by the California Department of Transportation (CalTrans) under PATH TO4204. The contents of this paper reflect the views of the authors who are responsible for the facts and accuracy of the data presented herein. The contents do not necessarily reflect the official views or policies of the State of California. This paper does not constitute a standard, specification, or regulation.

References

[1] Y. Bar-Shalom and T. E. Fortmann, "Tracking and Data Association", Academic Press, Inc., New York, NY, 1988

[2] T. Fujioka and M. Omae, "Vehicle following control in lateral direction for platooning", *Vehicle System Dynamics Supplement 28* (1998), pp. 422-437

[3] S. Gehrig and F. Stein, "A Trajectory-Based Approach for the Lateral Control of Car Following Systems", *Proceedings of the Intelligent Vehicles Symposium '98*, pp. 3596-3601, 1998.

[4] P. Hingwe, and M. Tomizuka, "Robust and gain scheduled H_∞ controllers for lateral guidance of passenger vehicles in AHS", *Proceedings of the ASME Dynamic Systems and Control Division*, DSC-Vol. 61, November 1997, pp. 707-713

[5] G. Lu and M. Tomizuka, "A Laser Scanning Radar Based Autonomous Lateral Vehicle Following Control Scheme for Automated Highways", *Proceedings of American Control Conference*, Denver, CO, 2003.

[6] D. Swaroop and J. K. Hedrick, "String Stability of Interconnected Systems", *IEEE Transaction on Automatic Control*, Vol. 41, No. 3, March 1996